

400 - 06

## CONTROL OF ACOUSTICALLY COUPLED COMBUSTION AND FLUID DYNAMIC INSTABILITIES

S. Raghu\* and K.R. Sreenivasan\*  
Mason Laboratory, Yale University  
New Haven, CT 06520

### Abstract

In this paper we discuss a set of methods for the active control of combustion and acoustically coupled fluid dynamic instabilities. These methods are based on the theoretical understanding of the interaction of mass, momentum and energy sources with a disturbance in the system. It is shown that this type of source-disturbance interaction could result in either amplification or decay of the energy in the disturbance depending on the phase relationship between them. We demonstrate successful control in several cases of fluid dynamic and combustion instability ranging from laboratory scale experiments to an operational, large combustion tunnel.

### 1 Introduction

Combustion instabilities are encountered in the development of almost all combustion systems, ranging from aircraft engines to ramjets and rocket propulsion systems regardless of the type of fuel used (gaseous, liquid or solid type). They manifest as large-amplitude pressure disturbances resulting in the generation of combustion noise. The noise generated can be of two types: a) Combustion roar, which has a broadband spectral content, and b) Resonant combustion noise having a discrete frequency content and generally of a much higher magnitude than the former. In addition to the large acoustic noise output from these instabilities there are several other consequences. To mention a few here, one may have unsteady combustion which could alter the reaction kinetics, or large amplitude pressure oscillations the extreme effect of which could be the extinction of the flame itself; the vibratory loads induced by these oscillations could also result in the structural failure of the components.

Such acoustic oscillations are not confined to combustion systems alone, and are known to occur even in purely fluid dynamic situations. An example is the 'whistler nozzle' phenomenon where a shear layer impingement on a solid edge provides the source of instability. Pure resonant tones are observed<sup>1</sup> even in jet flows under certain conditions of density ratio and Mach number.

There has been considerable effort toward understanding the phenomenon of combustion instability in the hope of designing quiet and stable combustion systems. The vast amount of literature devoted to this aspect of combustion bears evidence to the importance of the problem. A good review of the work done on the combustion instabilities can be found in references 2 and 3. The recent upsurge in the efforts towards aircraft noise control is also an indication of the importance of the problem even under purely fluid dynamic conditions.

This paper is devoted to the control of resonant combustion and fluid dynamic instabilities in which acoustic feedback plays a decisive role. We demonstrate experimentally a set of methods for the active control of such instabilities. These methods are based on the theoretical understanding of the interaction of mass, momentum or energy sources with a disturbance in the system.

The theoretical analysis is discussed in detail in ref. 4 and we mention only the primary result of the analysis here. We start with the

equations of motion of a fluid with mass, momentum and energy sources in the system and obtain the rate of growth of the disturbance in terms of the perturbed quantities. It can be expressed in the form

$$dE/dt + \nabla \cdot J = -\phi + \sigma \quad (1)$$

where  $E$  is the energy in the disturbance,  $J$  represents the rate at which the disturbance energy radiates from the system, and  $\phi$  is the dissipation term which includes losses due to viscosity, heat and mass diffusion and by chemical reactions. The last term, which we shall call the 'control term', is of immediate significance in the present context, and is given by

$$\sigma = \dot{m}' p' / \rho_0 + \mathbf{E}' \cdot \nabla' + \dot{Q}' T' / T_0 - T' / T_0 \sum_{i=1}^N \mu_{i0} M_i \quad (2)$$

It represents the energy addition/extraction through the interaction of the mass, momentum and energy sources with the perturbation quantities of the system. If this quantity is positive then energy is added to the disturbance, while the energy is extracted from it if the term is negative. Thus, by proper phasing of the mass, heat, momentum or species addition with the fluctuating pressure, velocity, temperature and chemical potential respectively, the amplitude of the disturbance energy in a system can be controlled.

Our method of control is based on the above principle; we explore the first three schemes i.e., heat, momentum and mass addition at proper phase with respect to the disturbance. While control may in principle be effected by species injection (i.e., the remaining terms in Eqn. (2), no attempt of such control will be discussed here. It should also be mentioned that we deal here with periodic disturbances, the advantage is that their phase of oscillation is tractable, which is essential to achieve the desired control action. An exception to this will be made in the case of a turbulent pipe flow where we demonstrate control of a large amplitude pressure perturbation superposed on background turbulence.

We note that the foregoing interpretation of eqn. (1) is strictly correct for linear perturbations only; however, with a suitable reinterpretation of the mass, momentum and heat sources, the same ideas can be useful even for highly nonlinear disturbances.

### II Method of Heat addition

Our work on the method of heat addition was reported in the previous paper<sup>5</sup>. We briefly summarize it here for the sake of completeness. It was shown that the growth or decay of the disturbance in a fluid with a heat source is governed by the expression

$$\int dE/dt d^3x = \int d^3x \dot{Q}'(\mathbf{x}, t) T'(\mathbf{x}, t) / T_0(\mathbf{x}) \quad (3)$$

The disturbance grows in time if the above quantity is positive and decays when it is negative. This method was used to control the oscillations in a Rijke tube, resonance in a pipe set up by a loudspeaker and the whistler nozzle oscillations. In all these cases an electrical heating coil was used for the purpose of heat addition and the appropriate phase for the desired control action was obtained by placing the heating coils at predetermined positions (based on the mode shape of oscillations) in the system. It was shown that the amplitude of oscillations could be reduced a thousandfold with as low as 10% of the heater power required to drive the oscillations and could be further reduced for longer 'waiting times' (time required for the oscillations to decay to a certain predetermined level). The additional temperature increase in all the above cases of control was less than 7% of the existing temperature in the system. We now demonstrate the same method for the control of oscillations with a superposed turbulent noise in the system.

\* Post Doctoral Associate

\* Professor, Department of Mechanical Engineering  
Member AIAA

©1987 by S. Raghu.

## Control of Pressure Oscillations in a Turbulent Pipe Flow

We examine in this section the control of acoustic standing waves generated in a pipe flow by the coupling of a shear layer instability with the organ-pipe resonance frequency of the system; the important difference between this example and the instances discussed in our previous paper is that the flow here is turbulent. The implications of the present experiments could be important since most of the practical flows are indeed turbulent in nature.

The experimental arrangement is shown in figure 1. It consists of a 185 cm long, 7 cm diameter pipe in which an annular ring of 3.3 cm diameter is positioned 5 cm from the upstream end of the pipe. This upstream end of the pipe is connected to a 9:1 contraction nozzle which in turn is connected to a large plenum chamber supplied with air by means of a centrifugal blower. Pressure oscillations were measured by means of a condenser microphone and the velocity signals by means of a hot-wire operated on a constant temperature anemometer (DISA 55M01). Mean velocity at the exit of the pipe was measured by means of a Pitot tube connected to a Betz manometer.

Four modes of oscillations could be set up in this arrangement, depending on the velocity at the exit of the pipe. Although we do not fully understand how these modes are set up, we may rationalize their occurrence in the following way. The dynamics of the shear layer at the annular ring is governed, among other things, by two factors: its natural instability, and the feedback of the pressure waves created by these instabilities. When the frequency of the shear layer roll-up coincides with one of the resonance frequencies of the pipe, there is a strong feedback of these pressure fluctuations to the shear layer, the rolling-up mechanism becomes more organized, thus setting up a standing wave of sizeable amplitude in the pipe. Table I shows the frequency of each mode and the centerline flow velocity at which it occurs.

TABLE I

Mode	I	II	III	IV
Frequency, Hz	100	200	260	340
Velocity, cm/s	100	420	540	890

The mode shapes were obtained by traversing the microphone from end to end. These are also shown in figure 1. Due to the inherent limitations of the experimental arrangement (i.e., poor heat resistivity of the pipe and the collar housing the heating coil), the major part of the experiments was confined to modes II, III and IV. Since the pressure signals for all these modes showed similar characteristics namely a periodic oscillation superposed over a broadband turbulent noise (as will be shown later), it was decided to study the control of mode IV oscillations in detail. Some results of the attempts to control the other mode oscillations will also be mentioned briefly.

The flow corresponding to the mode IV conditions was fully turbulent. The flow Reynolds number (based on the center-line mean velocity and the diameter of the pipe) was about 40,000. Figures 2a show a typical hot-wire trace of the streamwise velocity fluctuations  $u'$  and the power spectral distribution of  $u'$ . A particularly important observation concerns the absence of any discrete peaks in the power spectral density. The situation is much the same for other modes. We shall return to figures 2b subsequently.

Figure 3a shows pressure oscillations corresponding to mode IV, the frequency being 340 Hz. Note that this fundamental mode is randomly modulated by the fluctuating random flow field. The power spectral distribution of the pressure fluctuations is quite revealing: it shows a strong peak at around 340 Hz, although the 'background noise' is quite broad-band. One other comment worth making for later reference is that, in addition to the 340 Hz mode, the power spectral density shows a weaker peak at 200 Hz, corresponding to the fact that the 200 Hz mode (mode II) coexists with the 340 Hz mode, although the latter is stronger in energy by a factor of about 50. The pressure and the velocity signals corresponding to figures 2 and 3 were obtained at  $x = 104$  cm.

In order to obtain effective control, it is essential to know the response of the control heater in relation to the pressure oscillations in the system. This depends upon the phase of the velocity field around the heater, which in turn is governed by a definite phase relationship with  $p'$ ,  $u'$  leading  $p'$  by  $\pi/2$  when  $dp/dx$  is positive and lagging by  $\pi/2$  when negative.<sup>4</sup>

Now referring to the mode shape IV of figure 1, it is clear that the effect of positioning the heater in regions a-b, c-d, e-f, g-h must be similar, and opposite to locating the heater in the remaining of the positions. We thus decided to test the effect of the heater for two representative positions  $x=80$  cm and 160 cm. For modes II and IV, both these heater locations can be expected to have similar effects, while for mode III (260 Hz), the effects for these positions can be expected to be opposite. Keeping constant the electrical power input to the heater, we obtained the ratio of the mean square pressure with and without the control heater. Table II shows that there is generally a substantial reduction of the mean square energy when the heater is located at 80 cm, except for mode II for which it is only marginally effective since the heater location is not the optimal position for suppressing the oscillations. The 160 cm position, on the other hand, produces an attenuation for modes II and IV, but a reinforcement for mode III. It must be noted that the mean square of the velocity fluctuation showed no change for any combination of conditions. However, the filtered signals (at the appropriate mode frequency) showed a very slight reduction (of the order of a couple of per cent) whenever there was a reduction in the amplitude of pressure oscillations.

TABLE II

Mode	II		III		IV	
	80	160	80	160	80	160
$x$ , cm	80	160	80	160	80	160
Acoustic Power Ratio	0.96	0.55	0.16	1.5	0.4	0.61

Having shown that some degree of control is possible, we now plot in figure 4 the acoustic power (the ratio of that with control to that without control) as a function of the heating power supplied to the coil. (For these studies, two heating coils were placed one behind the other at  $x = 120$  cm.) It is clear that over a range of heating conditions, the amount of control is directly dependent on the amount of heating.

In figures 2a and 3a we showed the velocity and pressure signals and their power density distributions with no control. A comparison of these with the corresponding quantities with control is now discussed. The pressure trace of figure 3b (plotted to the same scale as in figure 3a) shows a large reduction in magnitude. The remainder of the pressure signal has two features worth mentioning. First, it is substantially more disorganized than that prior to control. Second, as the power spectral distribution of  $p'$  (figure 3a) shows, the most dominant mode that remains is not mode IV (340 Hz), but is a combination of modes II and III (200 and 260 Hz respectively). The reasons for this appear to be:

(a) The 200 Hz mode already apparent in figure 3a is not attenuated to the same extent as the 340 Hz mode, so that its relative prominence is increased;

(b) The relatively dormant 260 Hz mode was amplified by the heater.

These two observations effectively reflect upon the nature of the present method of control. Not all pressure fluctuations can be suppressed no matter how much the heating power is because modes previously dormant either stay unmitigated or in fact grow.

It must be remarked that, in contrast to the pressure oscillations, the velocity fluctuations do not undergo important changes. A comparison of velocity spectra with and without control (figure 2b) showed that the most important change was a relatively small reduction in amplitude at that frequency.

### Cross-Spectral Density Distributions of Pressure and Velocity Signals

Because of the complex nature of the flow field, the same degree of understanding as in the earlier examples of pure tone appears to elude us. Consequently, the problem in a turbulent environment cannot be as neatly pigeonholed. However, it has been clearly demonstrated here that pressure oscillations which are not pure-tone can indeed be suppressed by the heat addition technique even though the background flow is broadband. The likely reason for this is a possible existence of relatively strong cross-spectral correlation between the pressure and velocity fluctuations at the frequency of the most dominant pressure mode. To put this expectation on a firmer ground, we decided to measure the cross-spectral correlation between the pressure fluctuation  $p'$  and the velocity fluctuation  $u'$ . The cross-spectral correlation density is defined as

$$G_{pu}(f) = 2 \int R_{pu}(t) \exp(-i2\pi ft) dt, \quad 0 \leq t \leq \infty \quad (4)$$

where  $R_{pu}$  is the correlation function of  $p'$  and  $u'$ . Alternatively, it can also be defined as:

$$G(f) = 2 \lim_{T \rightarrow \infty} 1/T E [P_f^*(f, T) U_f(f, T)] \quad (5)$$

where  $E$  denotes the expected value (or mean) of the quantities within the parenthesis, and

$$P_f(f, T) = \int p'(t) \exp(-i2\pi ft) dt \quad (6)$$

$$U_f(f, T) = \int u'(t) \exp(-i2\pi ft) dt \quad (7)$$

are the finite Fourier transforms of the pressure and velocity fluctuations respectively.

It is seen from figure 5a that there is a strong correlation between the  $p'$  and  $u'$  signals at 200 Hz and 340 Hz, with that at 340 Hz being the strongest (about 2 orders of magnitude or more above the background value). With control, the correlation at 340 Hz becomes a little weaker (figure 5b), although it is still quite strong; that at 200 Hz seems to remain intact. This last fact suggests that with more power supplied to the control heater, the 200 Hz mode might also begin to decay.

To summarize, we have seen (from the current as well as our previous experiments) that the heater as a control device possesses two special qualities: (1) Selectivity or specificity -- that is, its ability to suppress selectively one or another acoustic mode by properly positioning the devices, and (2) Insensitivity -- that is, its action is not very sensitive to its exact location within the device. These qualities are expected to be shared by other devices of active control, because the criterion (eqn. 3) involves a spatial integration of the temporal correlations of a system fluctuation and a control fluctuation.

In all our experiments there is a large mean component of the heat addition which does not play any role in the control process, and therefore the efficiency of the control device is rather low. The conventional heat sources have a large thermal inertia and a compromise is required with the heat capacity requirements. Better methods of heat addition would eliminate this mean heat addition thereby improving the efficiency of the control device.

### III The Method of Force Addition

Analogous to the method of heat addition, the expression that governs the energy transfer by a momentum source is given by

$$\int \partial E / \partial t d^3x = \int d^3x \mathbf{F}' \cdot \mathbf{v}' \quad (8)$$

where  $\mathbf{F}'$  is the fluctuating external force added to the fluid volume and  $\mathbf{v}'$  is the velocity fluctuation in the system. The oscillations are suppressed if the value of the integral is negative and amplified if positive. External forces (as a source of momentum) can be generated by different ways -- centrifugal forces, magnetic forces and drag forces. In this discussion we confine ourselves to drag forces since that is the simplest to generate. Consider a cylinder around which there is a fluid flow. When a fluctuating velocity field exists in the

system, say  $\mathbf{v}'$  which varies as  $\mathbf{v}'_0 \exp(i\omega t)$ , then the drag can be written as  $D \exp(i\omega t + \phi)$  where the phase angle is a complex function of the velocity and the frequency of oscillation. Up to Reynolds number of the order of 1000, however, the phase relationship of the drag and the velocity is such that the value of the integral  $\int dt \mathbf{F}' \cdot \mathbf{v}' d^3x$  is negative<sup>6</sup> (i.e. there are no self excited oscillations),  $\mathbf{F}'$  representing the drag in the present case. This implies that the drag is sufficiently out of phase with the velocity, and in the case of a steady flow this phase difference should be exactly 180 degrees since it would be a function only of the velocity. This means that the sense of the drag vector is always opposite that of the velocity vector in the case of a steady flow. The fluctuating velocity field in a resonant type instability is created by the pressure oscillations in the system.

We choose the whistler nozzle arrangement to demonstrate the use of drag forces for suppressing the pressure oscillations. Resonance in the whistler nozzle is set up because of the upstream propagation of the disturbances generated due to the shear layer instability and the resulting coupling of the same with the resonance chamber. (For more details of the whistler nozzle see ref. 7) The experimental arrangement is shown in figure 6. The particular resonance chamber shown in the figure resonates in two different modes (within the velocity range of the present arrangement) for the two exit velocities of 9 m/s and 5 m/s. The resonance frequency for the former case is about 160 Hz (the 'high frequency mode') and 70 Hz for the latter case (the 'low frequency mode').

In the present study only mode II is studied except when the contrary is mentioned. Body force (drag) is generated by placing a fine screen in the pipe. This drag has a steady component due to the mean velocity of the flow in the pipe (~ 0.3 m/s) and a fluctuating part due to the periodic velocity fluctuations. The steady drag component does not contribute to the suppression of oscillations since the value of the integral  $\int \mathbf{F}' \cdot \mathbf{v}' dt$  over a cycle is zero. It is the unsteady part of the drag that contributes to the control of oscillations. This is analogous to the use of heating coils with a steady state output of heat in addition to the fluctuating heat release rate. Based upon the wire diameter of the screen and the mean velocity of the flow in the pipe, the maximum Reynolds number is about 9.0. The drag coefficient in this low Reynolds number regime can be approximated by the formula<sup>8</sup>

$$C_d \sim 1/Re \quad (9)$$

If the screen can be approximated by cylinders of finite length, then the total drag depends on the total length of the wire in the screen. Hence, the drag is a function of the solidity of the screen (where the solidity is the ratio of the blocked area to the unblocked area to the flow) and increases with the solidity. A solid disc of the same solidity would not produce the same effect however, for, it would alter both the fluid mechanical as well as the acoustical properties of the pipe. In our experiments, the drag is out of phase with the flow velocity by nearly 180 degrees as was experimentally determined<sup>9</sup>. Hence, the value of the integral of  $\mathbf{F}' \cdot \mathbf{v}'$  over a cycle is always negative and energy is extracted from the pressure oscillations in the pipe, the exact amount of energy extraction being proportional to  $\mathbf{F}'$ .

### Suppression of Oscillations using Stationary Screens

Three screens of different solidity were used in the experiments. The details of the screens are given in Table III.

TABLE III

Screen	Solidity	Mesh (cm)	Wire diameter (mm)
1	0.4	0.32	0.68
2	0.5	0.16	0.38
3	0.6	0.08	0.31

The screens were mounted on a thin annular plexiglass ring which was placed at different positions (velocity nodes and antinodes) to study their effectiveness. In our experiments, for mode II,  $x = 70.0$  cm and  $x = 160.0$  cm represent the velocity antinodes and  $x = 19.0$  cm and  $x = 115$  cm represent the velocity nodes (see figure 6). The

microphone was always placed at a distance of 37 cm (chosen arbitrarily) upstream from the exit of the jet. Figure 7 shows the comparison of the acoustic power at the resonance frequency when screens were placed at different locations in the whistler nozzle. It is also possible to see from the same figure the effectiveness of the various screens. The screen with the largest mesh (lowest solidity) has reduced the amplitude by half an order of magnitude when placed in the pressure node (velocity antinode, i.e., point of maximum velocity fluctuation). Screen 2 produces a slightly higher reduction, but the most dramatic effect occurs with the introduction of screen 3 where the oscillations are completely suppressed. The power spectrum shows a reduction of four orders of magnitude and the remnant signals are comparable to the background noise. One important point to note is that mere introduction of the screen into the pipe does not change the acoustic amplitude of oscillations, i.e., the effect of the screens is position sensitive; if the amplitude of the velocity fluctuations is minimum, the reduction in the amplitude of oscillation is also minimum and vice versa. A comparison of the power spectra of the pressure signals with no screen in the pipe with that of the screen 3 placed at  $x=19.0$  cm is also shown in figure 7. The effect of the other screens would be smaller than this because of their lower solidity (and hence lower drag). It is worthwhile mentioning that the acoustic mode shape is not altered by the introduction of the screens. Attempts were made to measure the pressure drop across the screens, but the drop was too small to be detected accurately by our instruments. A rough estimate showed a drop of about 0.7 % of the total head and hence there was no significant change in the mean velocity at the exit.

### Control by Oscillating Screens

Our next objective was to increase the effectiveness of the screens while minimizing the steady state component of the drag. In other words, we need to increase only the fluctuating component of the force (or drag in our case) since the steady component does not contribute to the suppression of oscillations ( $\int F \cdot v' dt$  is zero). Hence, if we oscillate the screen such that the relative fluctuating velocity component is increased, the fluctuating drag is also increased (since drag is proportional to the velocity). This was achieved by oscillating the screen antiphase (180 degrees) with the velocity fluctuations by means of a feedback system. The details of the oscillating mechanism are shown in figure 8. A loudspeaker to which a small (3mm) diameter piston was attached served as the oscillating mechanism. The diaphragm of the loudspeaker was removed in order to minimize the acoustic output of the speakers. This was done to minimize extraneous noise affecting the resonance in the whistler nozzle. The screen was mounted on two such pistons diametrically held by supports as shown. The pressure fluctuations in the pipe were sensed by a microphone and the phase of these signals could be varied before using them to drive the oscillating screen (but after amplification). Screen 2 was used in all the present experiments.

### a) Screens at pressure nodes

As mentioned before, the velocity fluctuations are maximum at these locations. The screen was positioned at  $x = 70$  cm. For suppression, the phase of the signal driving the screen with respect to the microphone signals was so adjusted to yield maximum reduction in amplitude, which corresponds to a phase shift of approximately 180 degrees between the velocity fluctuations and the screen velocity as determined by the phase characteristics of the oscillating mechanism. The results of suppression of oscillations are shown in figure 9(b), 9(a) being the no-control case. It can be seen that there is a reduction of about three orders of magnitude in the acoustic power of the fundamental frequency and the harmonics are completely suppressed.

We could also enhance the pressure oscillations by reducing the relative velocity of the fluctuations and hence the drag force. For this, the voltage signals driving the oscillating screens were approximately the inverse (a phase shift of 180 degrees) of that for suppression. The screen in this case was oscillated in phase with the velocity fluctuations, which amounts to addition of momentum in phase with the velocity fluctuation. The results are shown in figure 9(c). The

harmonics also show a small increase in amplitude.

### b) Screens at velocity nodes

In many practical situations the velocity antinodes may not be accessible for control purposes. This motivated the next part of our work, which is to control the oscillations from an arbitrary location in the flow field, the least effective location being the velocity node (minimum amplitude). Figure 10 shows the effect of control on the pressure oscillations, and, as can be seen, it was indeed possible to suppress the oscillations even from this location ( $x=19$  cm). The power spectrum of the pressure signal after suppression (figure 10b) is very similar to the corresponding one in case (a), i.e., figure 9b. However, a higher initial amplitude of oscillation of the screen was necessary for this purpose in order to generate the higher fluctuating drag. Figure 10c shows the amplification of signals when the screen is oscillated in phase with velocity fluctuations.

Attempts were also made to control the mode I oscillations. These oscillations are of a much larger magnitude (approximately 10 times the amplitude of mode I) and with the present design of the oscillating mechanism we were not able to suppress them completely. However, we could reduce the amplitude considerably by positioning the screen even at a velocity node ( $x=19$  cm). The velocity antinode was not accessible since it would be somewhere in the large settling chamber.

In this section we have demonstrated the use of force addition (drag forces in our case) to control pressure oscillations in a whistler nozzle, produced due to coupling between fluid dynamic instabilities and acoustic resonance. A stationary screen positioned at the proper location produces considerable reduction in the amplitude of oscillations, the exact amount of suppression depending upon the solidity of the screen; within the range of conditions we experimented, higher solidity resulted in greater reduction in amplitude. However, we have to pay the penalty of a higher net drag when we use higher solidity screens. In case of an oscillating screen the mean pressure drop for a given amplitude reduction is considerably reduced. It was also seen that in the latter case (oscillating screens) the control can be effected from ANY location in the pipe. The last result is of importance when practical applications are of interest.

### IV Control by Periodic Mass Addition

The control term associated with the mass source is the integral

$$\int dt \int m' p' d^3x \quad (10)$$

If the value of the integral is negative over a cycle, the energy in the disturbance decays in time and grows in magnitude otherwise. Periodic mass sources can be obtained by means of an applied periodic pressure gradient in a pipe or a channel flow, or by a variable area exit at the end of a mass flow source. In our experiments, the periodic mass flow was obtained by the variable area method which will be described in detail.

### Experimental arrangement

One of the simplest ways of obtaining resonant pressure oscillations in a pipe is to drive it by a sound source at its resonance frequency. Further, this system is less sensitive to a small additional air flow that is added during the periodic mass addition. In this context it should be mentioned that both the Rijke tube and the whistler nozzle are very sensitive to the air flow rates and the oscillations might naturally be suppressed by change of mass flux, and hence the choice of the above device for establishing pressure oscillations.

The experimental arrangement is shown in figure 11. It consists of a 150 cm long pyrex glass tube, 12.5 cm in diameter and open at both ends. A standing wave can be set up at its first fundamental mode by means of a loudspeaker placed at one end of the pipe and driven at the resonance frequency of the pipe. This

frequency is governed by the dimensions and the end conditions of the pipe. In our case, the tube is acoustically 'open' at both ends and hence the frequency  $f$  is given by<sup>10</sup>

$$f = C/2(L + 1.2a) - 100 \text{ Hz} \quad (11)$$

where  $C$  is the velocity of sound. The mode shape is also shown in figure 11. A 20 cm diameter loudspeaker placed at about 5 cm from one end of the pipe was used to drive the pipe to resonance. The pressure signals were sensed by a microphone placed in the middle of the tube. Through the other end of the pipe a periodic mass source, consisting of an air flow through a 1.9 cm diameter pipe with a variable area at the exit, is introduced. The pipe was supplied with air from a plenum chamber connected to a large compressor. The variable area slit was formed by two blades which could be oscillated in opposite directions to obtain a periodic mass flow. The inner pipe was 30 cm long (chosen arbitrarily) and the mass addition station was located (chosen for convenience of operation) at a distance of 15 cm from one end of the pipe. The velocity at the exit of the slit was about 22 m/s. The mass flow rate at this velocity was about 2.0 gm/s and the fluctuation was  $(2.0 \pm 0.75)$  and  $(2.0 \pm 1.5)$  gm/s. It was verified that the introduction of the inner pipe did not alter the mode shape in the pipe.

### The control system

The schematics of the control system are shown in figure 12. In the method of wave cancellation (figure 12a) the same signal generator drives both the loud speaker and the control device. The signal to the control device is however passed through a lock-in amplifier and a power amplifier to obtain the desired phase and amplitude. Pressure signals from the microphone (always placed at  $x = 75$  cm, this being the peak pressure position) were used for observing the effects of control. In case of the feedback method (figure 12b), the pressure signal from the microphone is the reference for applying the control. These signals are amplified and phase modified to be used for driving the control device. The loudspeaker is driven by an independent signal generator at constant phase.

It was first essential to determine the characteristics of the control device, i.e., the phase relationship of the displacement of the blade with respect to the input voltage. This was done by a fiber optic displacement transducer (MTI 1000 Photonic Sensor) which directly measures the displacement of the blade. At a frequency of 100 Hz the phase lag is about 20 degrees. The control device also has a limitation on its amplitude - it does not respond below a threshold voltage due to friction and has an upper limit of about 4.0 volts beyond which the displacement is nonlinear with respect to the input voltage.

### The Control

The control action depends upon the phase of the mass addition. Consider a large constant pressure ( $P$ ) chamber with an opening whose area varies as  $A \sin \omega t$ , where  $\omega$  is the angular frequency of variation. The exit velocity at the opening is determined by the pressure difference  $(P_0 - P_a)$ , where  $P_a$  is the ambient pressure and is given by

$$P_0 - P_a = 1/2 \rho v^2 \quad (12)$$

The mass flow rate is given by

$$\dot{m} = v A \sin \omega t \quad (13)$$

It was estimated that the variation in  $P_a$  brought about by the acoustic fluctuations was very small compared to  $P_0$  and therefore  $P_a$  is assumed to be constant in our experiments. The area variation was brought about by the moving blades (minimum area when the blades are closest and vice versa) and could be determined by knowing the displacement characteristics of the control device. The oscillations could be suppressed by two methods as described below.

### a) Method of Wave cancellation

In this method the same signal source is used to drive the loudspeaker as well as the blades forming the variable area slit. The phase of the signal supplied to the oscillating blades is however adjusted (approximately 180 degrees out of phase with the pressure signals) until the oscillations are completely suppressed. A constant amount of energy is expended every cycle in adding the mass to the system (the amplitude of  $m'$  is the same every cycle) and hence the control is of the open loop type. If the signal to the slit blades were inverted with respect to the above phase, the oscillations are amplified. Both results are shown in figure 13. This method is similar to the one used by Strykowski and Sreenivasan<sup>11</sup> for the suppression of Tollmien-Schlichting waves.

### b) Method of Feedback

In this method the pressure signals obtained from the microphone are modified (in both phase and magnitude) and used to drive the control device. Control (either suppression or amplification of oscillations) was achieved by visually adjusting the phase of the voltage signals driving the oscillating blades. The effect of control is shown in figure 14. Measurements using a Sound Pressure Level (SPL) meter indicated that there was a 15 dB reduction in the SPL when the oscillations were suppressed. Both the superposition and the feedback methods are equally effective in controlling the oscillations; the reason for a larger peak at the resonance frequency in the power spectrum of the pressure signals for this method of suppression as compared to the direct method (figure 13) is due to

inherent mechanical limitations of the oscillating mechanism. The blades do not oscillate below a certain threshold amplitude due to friction in the sliding parts; hence, until oscillations are of a certain magnitude - enough to generate a voltage beyond the threshold value - the feedback does not function and therefore oscillations up to a certain magnitude existed always. This problem is not encountered in the direct method because the blades were always driven by an external source whose magnitude did not depend on the oscillation amplitude. However, the present set up slightly differs from the ideal case since we use a constant-energy external source (loudspeaker) to drive the oscillations and this source of instability does not form a part of the feedback loop. In the method of feedback, the energy required decreases in every cycle and no energy is expended once the oscillations are completely suppressed.

We are thus able to demonstrate the use of periodic mass addition to control the resonance set up in a pipe by a loudspeaker. Although both methods of control (superposition and feedback) are equally effective in suppressing the oscillations, the feedback is a more efficient way of control since it not only suppresses the oscillations but also prevents them from attaining large amplitudes again. The energy required is also minimal since the amplitude of control action ( $m'$ ) decreases every cycle and is minimal once the oscillations are suppressed (below a threshold value). In the wave cancellation method a constant amount of energy is being supplied to the oscillating blades every cycle and the extent of control depends upon the amplitude of mass addition, since the resultant of two waves superposed is their algebraic sum at any instant. Hence, we need to know the exact amplitude *a priori* or else the corrective action can itself result in pressure oscillations if its amplitude exceeds that due to the instability.

### V Control of Organ-Pipe Oscillations in a Combustion Tunnel

Often, in real systems, the magnitude of the pressure fluctuations is so large that it might be desirable to use a combination of the previously mentioned methods to control the oscillations effectively. One such instance is the organ-pipe type oscillations that occur in a combustion tunnel. Note that control can also be effected from several stations in the systems, as long as the phase of the oscillations can be determined at these locations. In this section we describe a direct application of our methods established in the previous chapters to control oscillations in the combustion tunnel at

the Aero Propulsion Laboratory, Wright Patterson Air Force Base.

The details of the facility are reported elsewhere <sup>12</sup>. A schematic of the facility is shown in figure 15. A 2.5 gal/hr, 60 degree spray angle nozzle was used to inject the liquid JP-4 into a swirling, recirculating air flow. The primary swirl air flow was maintained constant throughout the experiments. The acoustic characteristics of the tunnel are governed by the length of the tunnel from the burner to the end of the tail pipe (which is about 5.3 m), and the dominant frequency during the tunnel run was about 100 Hz and the mode shape which was determined by a traversing microphone is also shown in figure 15.

### Method of control

In the present case, two 80 mesh screens (solidity of about 0.7) were positioned at the velocity antinodes (the velocity fluctuations are maximum at the antinodes). These screens had to be properly reinforced (by clamping the edges tightly between two metal bands) due to the high velocity in the tunnel (30 m/s). The mesh size was arrived at by the blockage and the drag considerations of the screens - lower mesh size screens could not suppress the pressure oscillations satisfactorily while higher mesh screens would cause large pressure losses in the system. In addition to the screens, four commercially available heating coils (20 cm in diameter and 2300 watts each) were positioned at  $x=290$  cm. This position corresponds to the location where the heat addition discourages the pressure oscillations. A thin steel wire screen of 45 mesh was sandwiched between each pair of heating coils to have uniform heat release in the whole cross-section of the tunnel.

### Instrumentation

A Bruel and Kjer sound pressure level (SPL) meter was used to measure the SPL of the tunnel noise during combustion. The instrument was placed at  $x = 356$  cm and approximately 70 cm from the center line of the tunnel. All measurements were made in the linear scale setting. Two Kistler pressure transducers (Type 211B5), mounted at  $x = 18$  cm and  $x = 127$  cm on the walls of the tunnel, were used to measure the pressure fluctuations inside the tunnel. The output from the above instruments was also connected to a Nicolet Spectrum Analyzer and an x-y recorder.

Typical power spectrum plots of the pressure signals for the cases of resonance and quiet running are shown in figure 16. Note that during instability strong peaks occur at the fundamental resonance frequency as well as its harmonics. These oscillations were audible as soon as they were above the flow noise. In our case flow noise was around 96 dB. During oscillations (without control) the sound pressure level (SPL) went up to about 116 dB, i.e., an increase of up to 20 dB, and occurred for almost the entire range of operating conditions of the tunnel as shown in figure 17. With the addition of the screens and the heat source at the appropriate places (as mentioned in Section III), there was significant improvement in the performance of the tunnel as seen in the stability margins of the figure 17. The stability boundary extends over a significant part of the operating range of the tunnel. Further, even when oscillations occurred with control, the SPL was much lower than the corresponding value without control. The maximum SPL with control was about 106 dB as compared to a maximum of 116 dB without control (see fig. 18) and the harmonic content was significantly reduced.

High-speed movie pictures of the flame indicated a highly organized vortex motion in the flame. The large pressure oscillations are seen to produce periodically shed vortices from the lip of the burner shroud. This causes a periodic variation in the flame front which is responsible for the periodic heat release rate as was confirmed from the luminosity measurements. This periodic heat addition serves as the instability sustaining mechanism in the system; however, the instability triggering mechanism could be different and is not clearly known in the present system.

By using a combination of the methods of force and heat addition, the organ-pipe type oscillations in the combustion tunnel were completely eliminated over a significant range of the operating conditions. Even in the regions where the oscillations persisted, the sound pressure level was reduced by at least 10 dB, which is a significant reduction in the combustion noise. The high-speed movies give us a physical insight into the strong interaction of the flame with the pressure oscillations-- a strong organized vortex motion responsible for the periodic heat release rate is produced at the burner due to these oscillations, and with control, this interaction is significantly reduced.

## VI Discussion and Conclusions

The objective of the present research has been to demonstrate the application of the generalized Rayleigh criterion as a rational tool for the control of combustion instabilities. The control term as given by eqn. 2 is

$$\sigma = \dot{m}'p'/\rho_0 + \dot{E}'/\gamma' + \dot{Q}'T'/T_0 - T'/T_0 \sum_{\lambda=1}^N \mu_{\lambda} M_{\lambda}$$

From each term on the RHS of the above equation a distinct method of control can be attained, i.e., periodic mass, force, heat and species generation. The last method, the generation of the chemical species against the appropriate chemical potential, has not been explored in the present work. The use of the first three methods however has been successfully demonstrated in several cases of combustion and fluid dynamic instabilities. In all these methods it has been shown that the instabilities could either be amplified or suppressed depending upon the desired control action. Some of the instability examples chosen are typical of combustion systems such as rockets and missiles, ramjets and even industrial and house-hold burners.

In the method of heat addition, the periodicity of the heat flux is dependent upon the velocity field in the system; needless to say that there is a large steady state component of the heat. This is because the heating coils had a high thermal inertia (it would take a long time for the coils to attain a steady state temperature) and therefore purely periodic heat addition could not be effected. Since the experiments were designed for the purpose of demonstration of the method, the heating coils were made from the materials available at hand and hence are less efficient as a control device. By the design of a proper heat addition device we estimate that the energy requirements for control will be reduced significantly. This is also necessary to minimize the additional temperature increase due to control particularly when there is a thermal constraint in the system. An attempt in this direction was made <sup>13</sup> where a quick response (low thermal inertia) heat source made of a grid of nichrome wire was constructed. It was found that the 'waiting time' was reduced by a factor of two in certain cases. Also, in many instances it might be desirable to use non-intrusive heat addition methods. Our immediate research is directed towards such a design. On similar lines as periodic heating, periodic cooling for suppression of oscillations is also being explored. In certain solid propellant rocket instabilities, the addition of aluminium particles have been found to change the characteristics of combustion <sup>14</sup>. Such a behavior could be attributed to modification of the phase of the heat release rate by the addition of these particles. A systematic study of this phenomenon would aid in the understanding and control of the solid propellant rocket instabilities.

In instances where the resonant instabilities are due to a local heat addition, that is, if the heat source is located in a place where periodic heat addition aids the build up of oscillations, it might be possible to prevent oscillations by means of redistributing the heat sources uniformly in the system. Such a redistribution could be made possible by design of fuels where a part of the fuel has a ignition time delay (such that it burns at a station downstream compared to the main combustion zone). In liquid fuels this effect can be brought about by merely having two different sizes of fuel droplets.



In the second method, external forces for the control of oscillations have been obtained by means of the fluid dynamic drag. At very low Reynolds number, the drag is directly proportional to the length of the wire in the screen. Hence, for a larger fluctuating drag, the screens have to be of a higher mesh, which means an increased steady state drag. This steady state drag does not contribute to the suppression of oscillations, but results in pressure loss in the flow. By oscillating the screen in the proper phase we were able to increase the effectiveness of the screen, i.e., we could use a lower mesh screen for the same amount of amplitude reduction as that of a rigidly fixed screen of higher mesh size. Therefore, in this method we have been able to control the phase of the interaction between the drag and the velocity fluctuations in contrast to the method of heat addition where the phase is controlled by the heat release characteristics of the control heat source. Other methods of force addition like centrifugal forces and magnetic forces need to be explored if non-intrusive devices are needed to suppress the oscillations.

The method of mass addition was used for the suppression of oscillations driven by a loudspeaker. Even in this case we had to have a steady component of the mass flow rate over which there were fluctuations superposed. This was so because the amplitude of the blade oscillations was limited by device constraints. Better devices could eliminate the steady mass flow and hence make the control more efficient. This method could be immediately incorporated to control the oscillations in after-burners, ramjets, etc., where there is plenty of secondary air being injected into the combustion chamber for cooling purposes. The phase relations were also verified by considering the response characteristics of all the components in the control system. Phase controlled periodic suction as a means to suppress the oscillations is yet to be explored.

It has been demonstrated that these methods of control can be used in combination when the oscillations are too large and one method alone is insufficient to suppress the oscillations. Also, control can be applied from several locations as long as the phase relations are known. An important feature of our method is that it is independent of the source of instability or the driving mechanism. It has varied from flame-driven oscillations in case of the Rijke tube and the combustion tunnel, shear layer impingement in case of the whistler nozzle and the pipe flow, the latter two being essentially fluid mechanical, and the loudspeaker driven oscillations in the pipe. Further, the choice of the control method, i.e., use of any of the methods for a given system has been demonstrated. For example, the loud speaker driven oscillations could be suppressed by either heat or mass addition and the whistler nozzle oscillations were suppressed by heat or body force addition. The choice of the control method in a real situation is of course governed by the temperature, pressure loss, mass flow and other constraints in the system.

One important point to bear in mind in the application of all these methods of control is the knowledge of the response characteristics of the control device itself. This is essential in order to implement the desired control effect in the control system. The question to ask is whether the control system has the desired frequency and amplitude response. At higher frequencies mechanical control systems have drawbacks due to their inherent inertia and hence we need other methods of control like laser induced pressure pulses, microwave heating, etc. The possibility of controlling the oscillations by applying the control action at a reduced frequency (say  $f/2$ ) should also be explored.

In the present work we have dealt with only the longitudinal modes of oscillations. Transverse and azimuthal modes of instability are also known to occur in combustion chambers. The same method of control should in principle be possible even for these modes. The problem arises only when the standing wave is not stationary but oscillates randomly around a mean position (as has been observed in some cases of ramjet instability). From our earlier results we have seen that the control is insensitive to a wide range of positions of the control heater, which implies that as long as the phase criterion

$$|\phi| > 90^\circ$$

(where  $\phi$  is the phase difference between the heat release rate and the pressure fluctuation) is satisfied the oscillations are discouraged. Hence small changes in the phase of heat, mass or momentum addition do not alter the desired control effect. This is in direct contrast to the wave cancellation technique where the phase relationship is crucial for the oscillations to be cancelled.

Our method of control should hold good for propagating waves as well, but the difficulty comes in the tracking the phase of every propagating wave to effect control. However, it should be remembered that it is the resonance that leads to the build up of the large amplitude of oscillations, and a small-amplitude propagating pressure wave may not cause as serious a damage as that of a resonant instability. Also, the method outlined can be extended to finite amplitude waves as well, and is clearly at an advantage since the wave cancellation technique is not a possibility here.

### Acknowledgements

The authors like to acknowledge the fruitful discussions we had with Prof. B.T. Chu during the course of this work. SR is grateful to Mr. R.P. Bradley and Dr. W.M. Roquemore of Aero Propulsion Laboratory, Wright Patterson Air Force Base, Ohio for their help in conducting experiments in their Combustion Tunnel Facility. We thank the AFOSR for the financial assistance provided for this work.

### References

1. David Kyle, "Absolute Instability in Variable Density Jets", Report 86FM6, Mechanical Engineering Department, Yale University, 1986.
2. Section I and II on Combustion Instability, Twelfth Symposium (International) on Combustion held at Poitiers, France, 1969, pp. 85-211.
3. Harje, D.T. and Reardon, F.H., (eds.), "Liquid Propellant Rocket Combustion Instability", NASA SP-194, 1972.
4. Chu, B.T., Sreenivasan, K.R. and Raghu, S., "On the Control of Combustion Instability", to appear in Progress in Aerospace Sciences.
5. Sreenivasan, K.R., Raghu, S. and Chu, B.T., "The Control of Pressure Oscillations in Combustion and Fluid Dynamical Systems", AIAA Shear Flow Conference, Boulder, Colorado, 1985.
6. Tanida, Y., Okajima, A. and Watanabe, Y., "Stability of a Circular Cylinder Oscillating in a Uniform Flow or in a Wake", Journal of Fluid Mechanics, Vol.61, part 4, 1973, pp. 769-784.
7. Hussain, A.K.M.F. and Hasan, M.A.Z., "The 'Whistler Nozzle' Phenomenon", Journal of Fluid Mechanics, Vol. 134, 1983, pp. 431-458.
8. Tritton, D.J., "Physical Fluid Dynamics", Van Nostrand Reinhold, 1984.
9. Raghu, S., "Control of Combustion and Acoustically Coupled Fluid Dynamic Instabilities", Ph.D. Thesis, Yale University, 1987.
10. Kinsler, L.E., et al, "Fundamentals of Acoustics", John Wiley and Sons, 1982.
11. Strykowski, P.J. and Sreenivasan, K.R., "The Control of Transitional Flows", AIAA Shear Flow Conference, Boulder, Colorado, 1985.
12. Roquemore, W.M., Britton, R.L. and Sandhu, S.S., "Dynamic Behaviour of a Bluff-Body Diffusion Flame", AIAA Journal, Vol.21-10, 1983, pp. 1410-1417.
13. Vogel, B., "The Design of a Heating Coil for the Control of Rijke Tube Oscillations", Project Report, Yale University, 1984.
14. Barrere, M. and Williams, F.A., "Comparison of Combustion Instabilities found in Various Types of Combustion Chambers", Twelfth Symposium (International) on Combustion held at Poitiers, France, 1969, pp. 169-181.

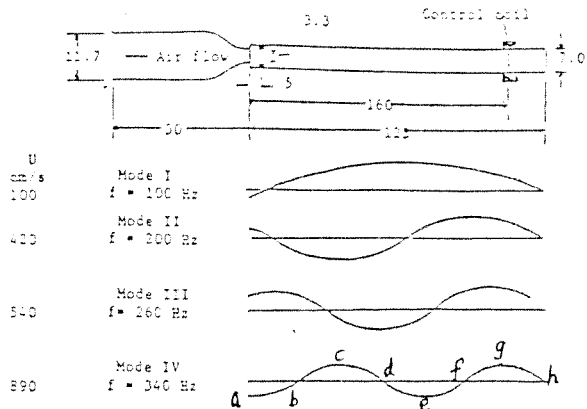


Figure 1. Schematic of the experimental apparatus and the mode shapes of resonance in the turbulent pipe flow arrangement. All dimensions are in centimeters.

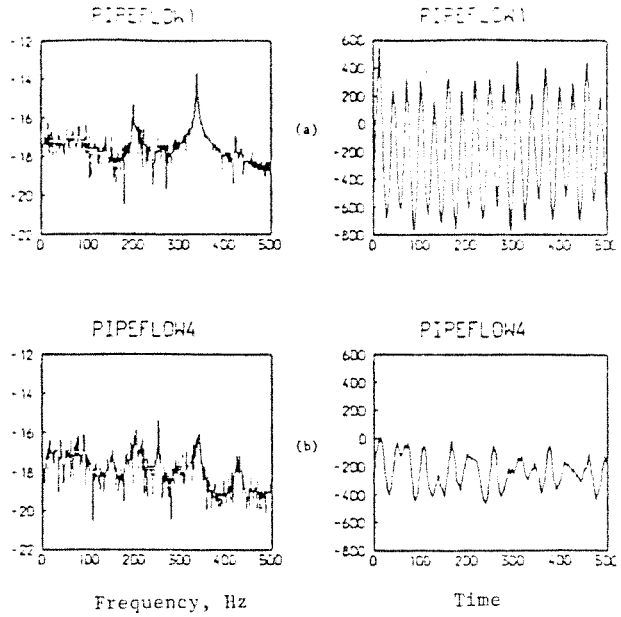


Figure 3. Pressure signals and spectral densities in the pipe. (a) no control, (b) with control.

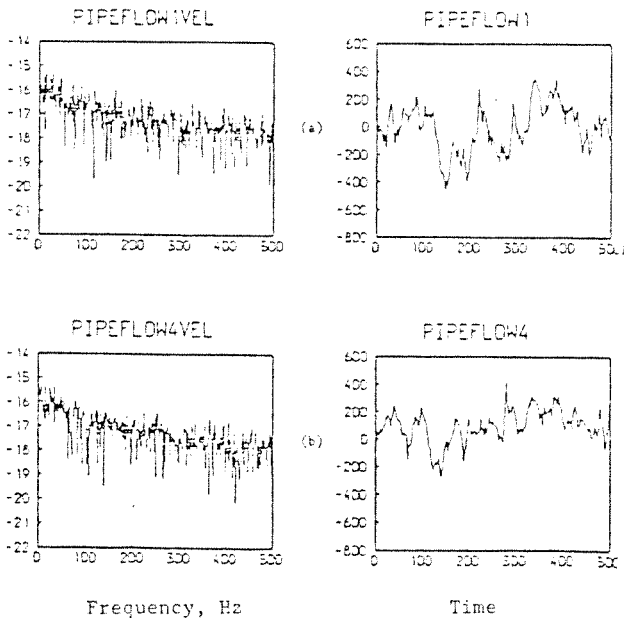


Figure 2. Velocity signals and spectral densities in the pipe: (a) no control, (b) with control.

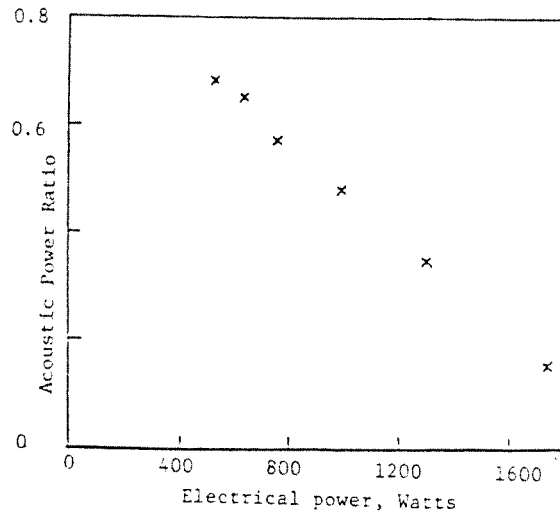


Figure 4. The ratio of acoustic power with control to without control as a function of the power supplied to the control heater located at 160 cm in the pipe.



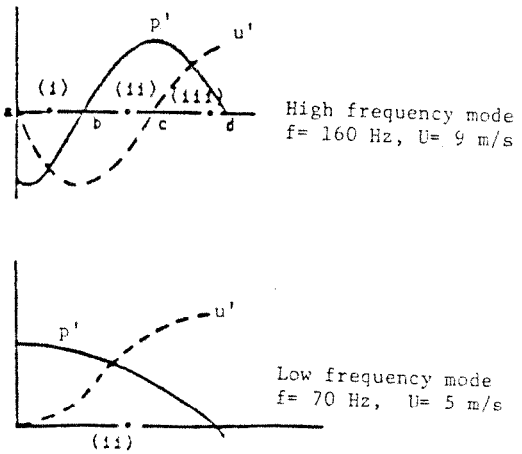
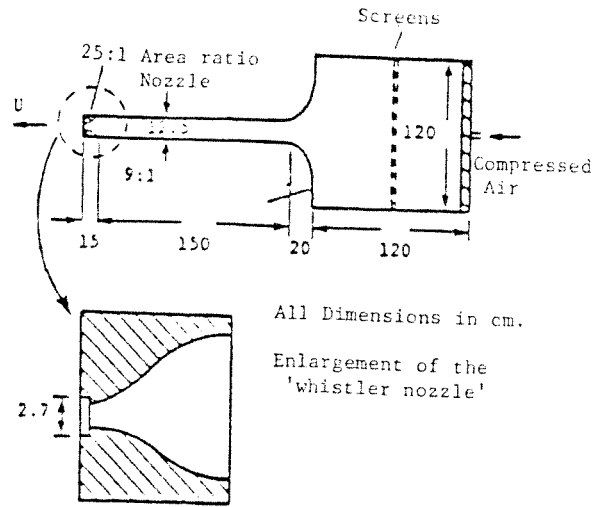
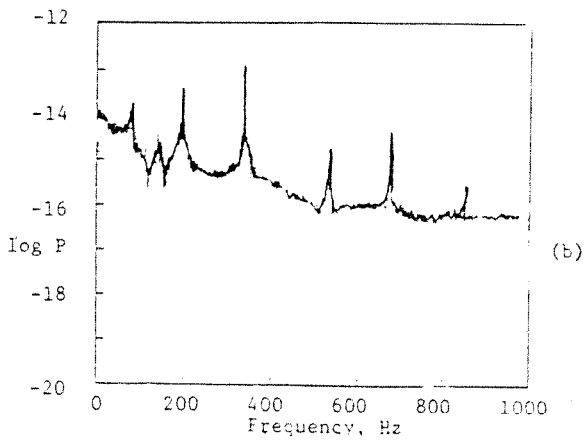
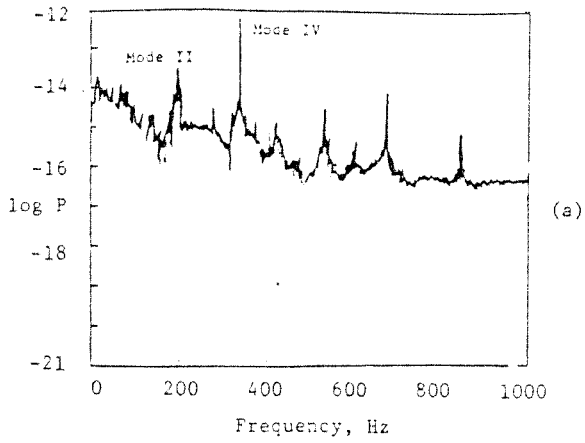


Figure 5. The cross-correlation between the pressure fluctuation  $p'$  and the velocity fluctuation  $u'$  in the pipe. Notice that the most dominant correlation comes at mode IV but there is a substantial correlation also at mode II. (a) no control, (b) with control.

Figure 6. The Whistler nozzle apparatus with the details of the 'whistler nozzle' and the mode shapes.

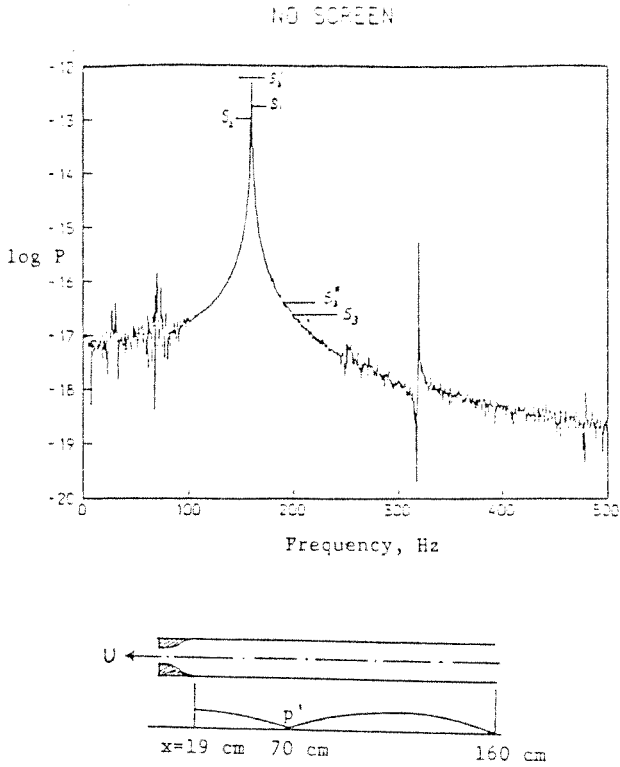


Figure 7. Comparison of the effectiveness of different screens.  $S_3$ : Screen 3 at  $x=70$  cm;  $S_2$ : Screen 2 at  $x=70$  cm;  $S_1$ : Screen 1 at  $x=70$  cm;  $S_3'$ : Screen 3 at  $x=19$  cm;  $S_3''$ : Screen 3 at  $x=160$  cm.

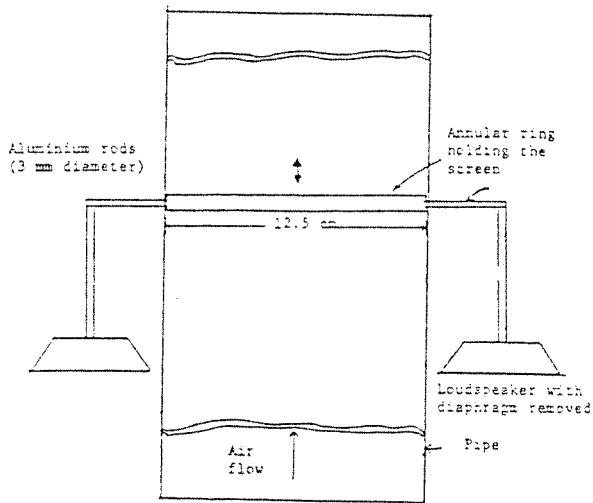


Figure 8. Oscillating screen arrangement in the whistler nozzle.

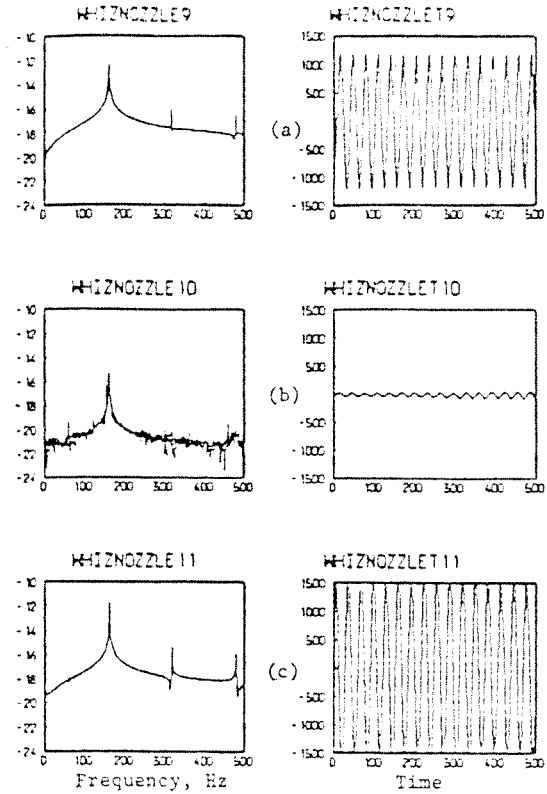


Figure 9. Power spectrum and time traces of pressure signals in the whistler nozzle for (a) no control, (b) suppression and (c) amplification. Screen located at  $x = 70$  cm.

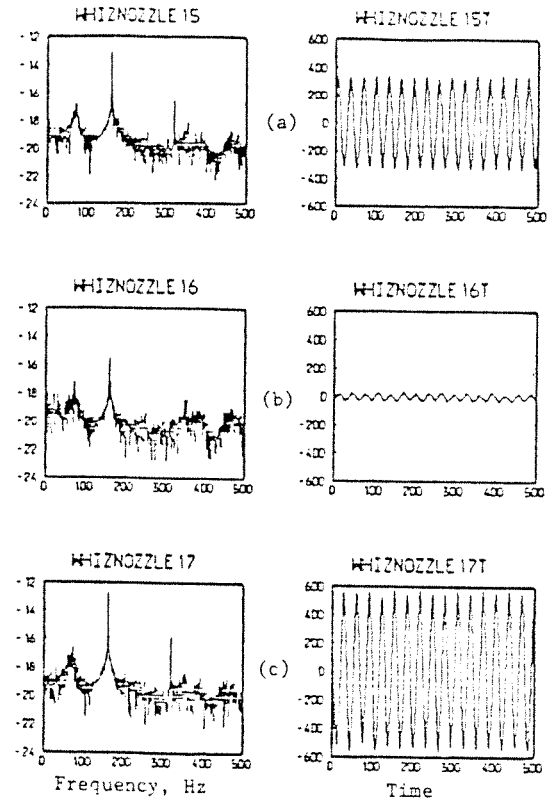


Figure 10. Power spectrum and time traces of pressure signals in the whistler nozzle for (a) no control, (b) suppression and (c) amplification. Screen located at  $x = 19$  cm.

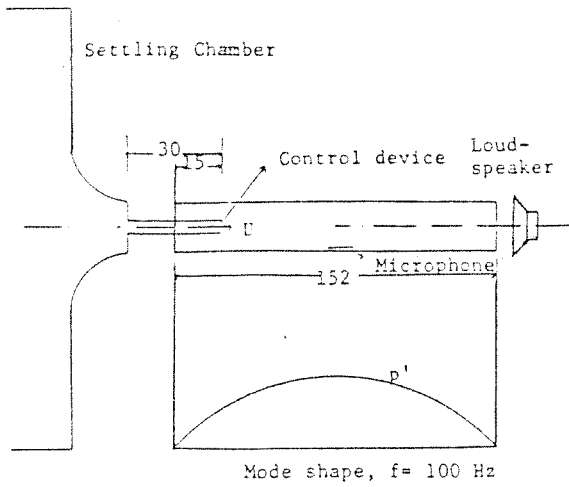


Figure 11. Arrangement for the periodic mass addition experiment and the mode shape of oscillations set up in the pipe. All dimensions are in centimeters.

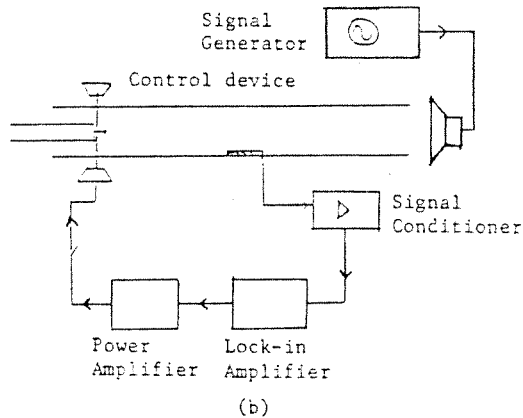
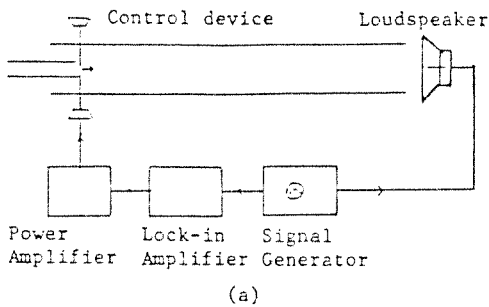


Figure 12. Details of the control system. (a) Direct method, (b) Feedback method.

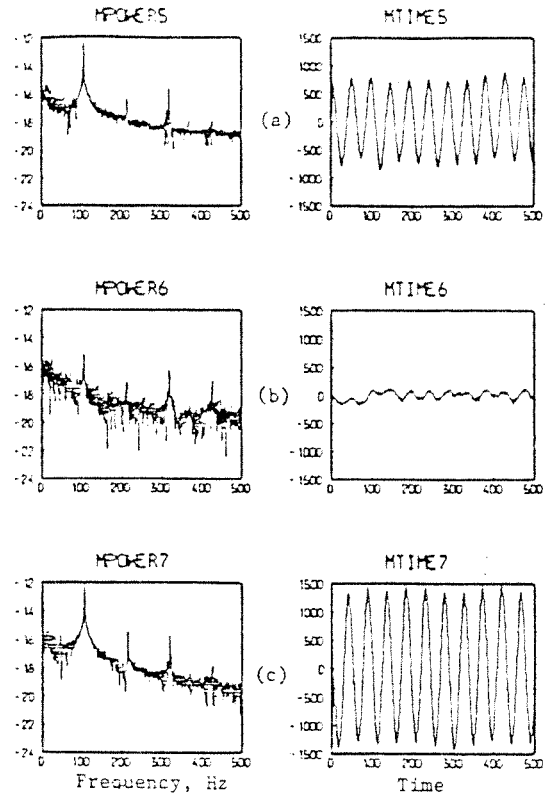


Figure 13. Pressure signals in the pipe during control by direct method. (a) No control, (b) Suppression and (c) Amplification.

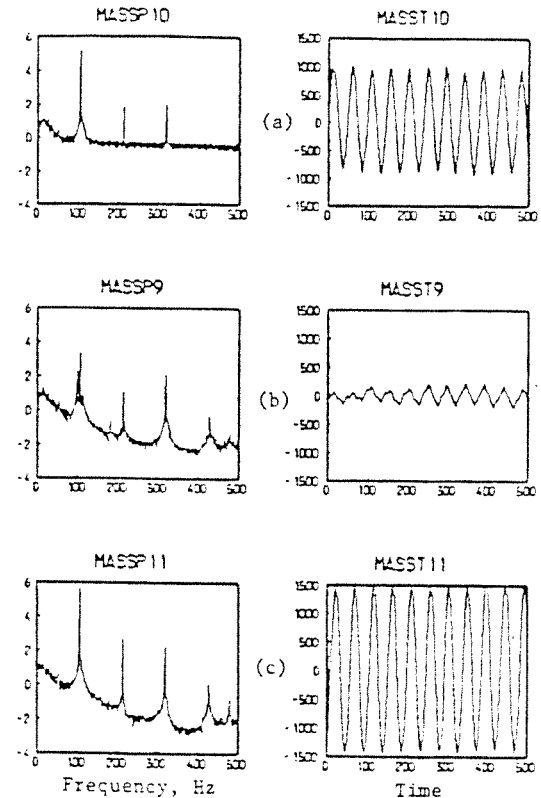


Figure 14. Pressure signals in the pipe during control by feedback method. (a) No control, (b) Suppression and (c) Amplification.

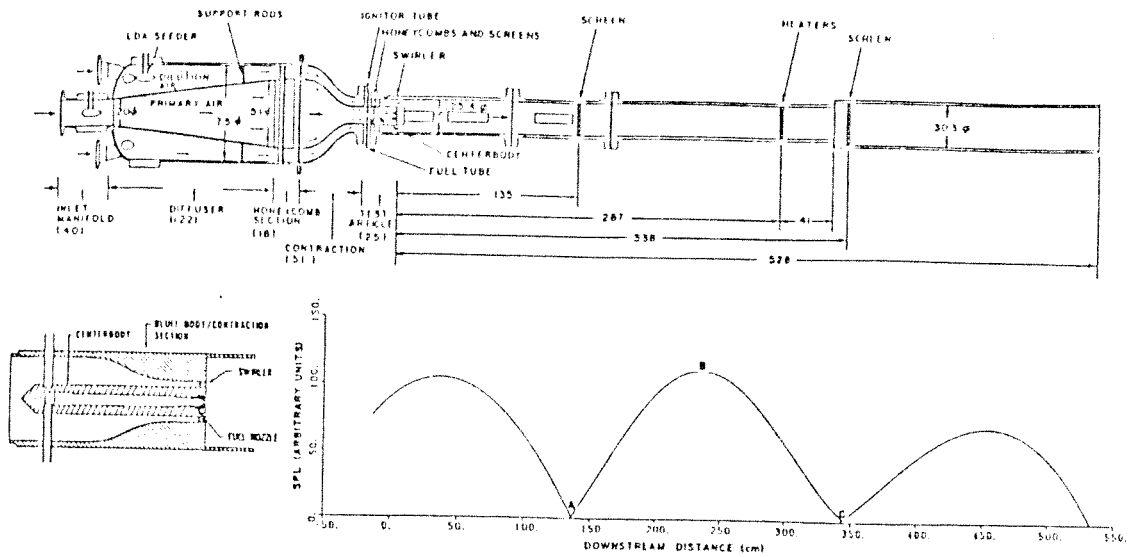


Figure 15. Combustion tunnel facility and the mode shape for the fundamental resonance frequency. Dimensions are in cm.

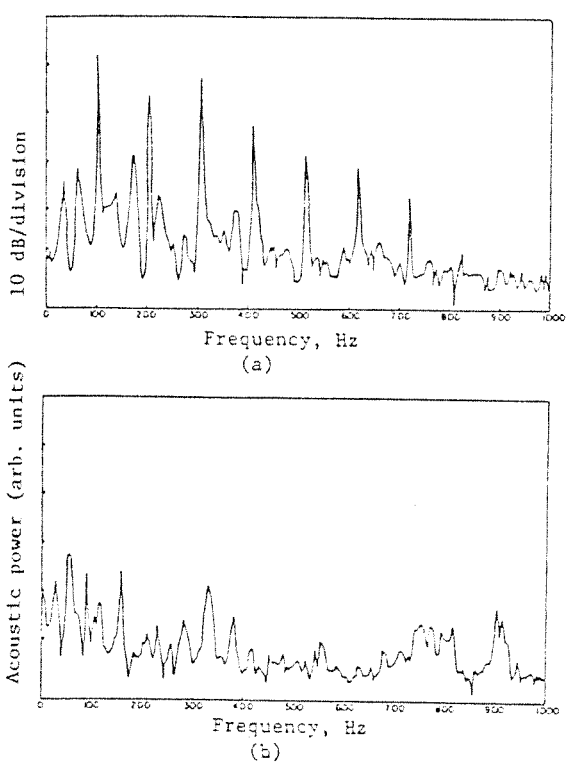


Figure 16. Power spectrum of the pressure signals in the tunnel during (a) resonant combustion (b) combustion without oscillations.

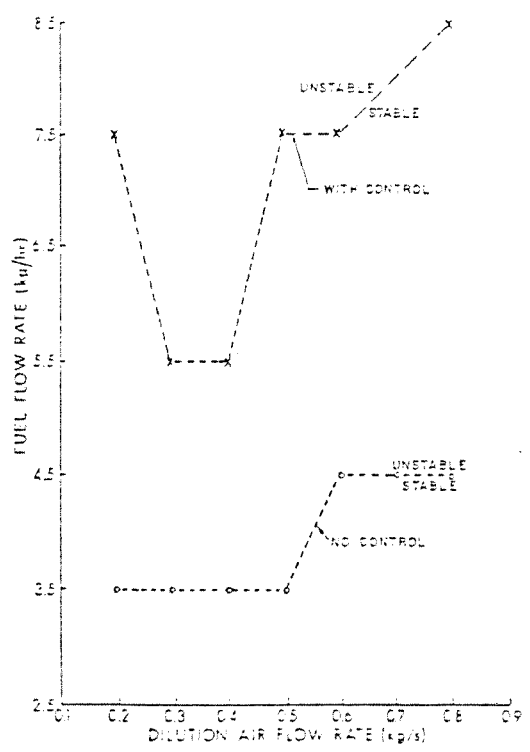


Figure 17. Stability margin of the tunnel with and without control.

